Electronic Supplementary Material (ESI) for Nanoscale.

– Supplementary Information –

Black Phosphorus Nanoelectromechanical Resonators Vibrating at Very High Frequencies

Zenghui Wang[1], Hao Jia[1], Xuqian Zheng[1], Rui Yang[1], Zefang Wang[2], G. J. Ye[3], X. H. Chen[3], Jie Shan[2], Philip X.-L. Feng[1,*]

[1]*Department of Electrical Engineering & Computer Science, Case School of Engineering, Case Western Reserve University, 10900 Euclid Avenue, Cleveland, OH 44106, USA*

[2]*Department of Physics, College of Arts & Sciences, Case Western Reserve University, 10900 Euclid Avenue, Cleveland, OH 44106, USA*

[3]*Hefei National Laboratory for Physical Science at Microscale and Department of Physics, University of Science and Technology of China, Hefei, Anhui 230026, China*

Table of Contents

[*]Corresponding Author. Email: philip.feng@case.edu

S1. Black Phosphorus (P) Resonator Fabrication

In order to fabricate high quality suspended black P nanoelectromechanical resonators, we transfer black P flakes onto Si/SiO_2 substrates with pre-patterned features using a dry transfer technique specially developed and optimized for black P. Upon surveying the different existing 2D material transfer methods[1,2,3] and evaluating their respective strengths, we adopt their good features and incorporate special steps uniquely developed to facilitate fast transfer of black P, in order to minimize the material's exposure to the ambient. We first cut a small rectangular piece from PDMS film (Fig. S1a), gently peel off the protection layers on both sides (Fig. S1b), and carefully stamp it onto a clean glass slide (Fig. S1c). The black P samples are then exfoliated for dozens of times (Fig. S1d) before we press the tape onto the PDMS stamp, and gently brush the surface using a Q-tip (Fig. S1e). Black P flakes transferred onto the PDMS stamp are quickly yet carefully inspected under optical microscope to identify promising black P flakes for device fabrication, and stored in vacuum chamber immediately afterwards. By keeping the black P flakes in vacuum chamber, we have sufficient time to carefully plan for the transfer: specifically, we choose the best substrate with the most suitable pattern that fits the size and shape of the black P flake; we determine the optimal substrate mounting orientation, and we preview and examine the expected device geometry by overlaying optical images of the black P flake and the substrate in computer, in order to determine the best transfer strategy. In this way, the time duration of black P exposed to ambient environment during the transfer process is minimized, which helps prevent material degradation.

As soon as the transfer strategy is planned, we mount the pre-patterned substrate and clamp the glass slide with desired black P flake on its PDMS to our custom-built transfer stage (Fig. S1f). We move the black P flake to the target area with the micro-manipulator and align the flake with the substrate pattern

under the microscope (Fig. S1g). As we gradually lower the glass slide to bring the PDMS stamp and substrate into contact (Fig. S1h), we keep fine-adjusting the position and microscope focus so that the black P flake exactly covers the desired microtrenches and electrodes. After the entire black P flake is in contact with the substrate, we gently lift up the glass slide, leaving the black P flake on the substrate by van der Waals forces (Fig. S1i). The resulting device is perfectly suspended over the microtrench and in direct contact with the metal electrodes underneath (Fig. S1j).

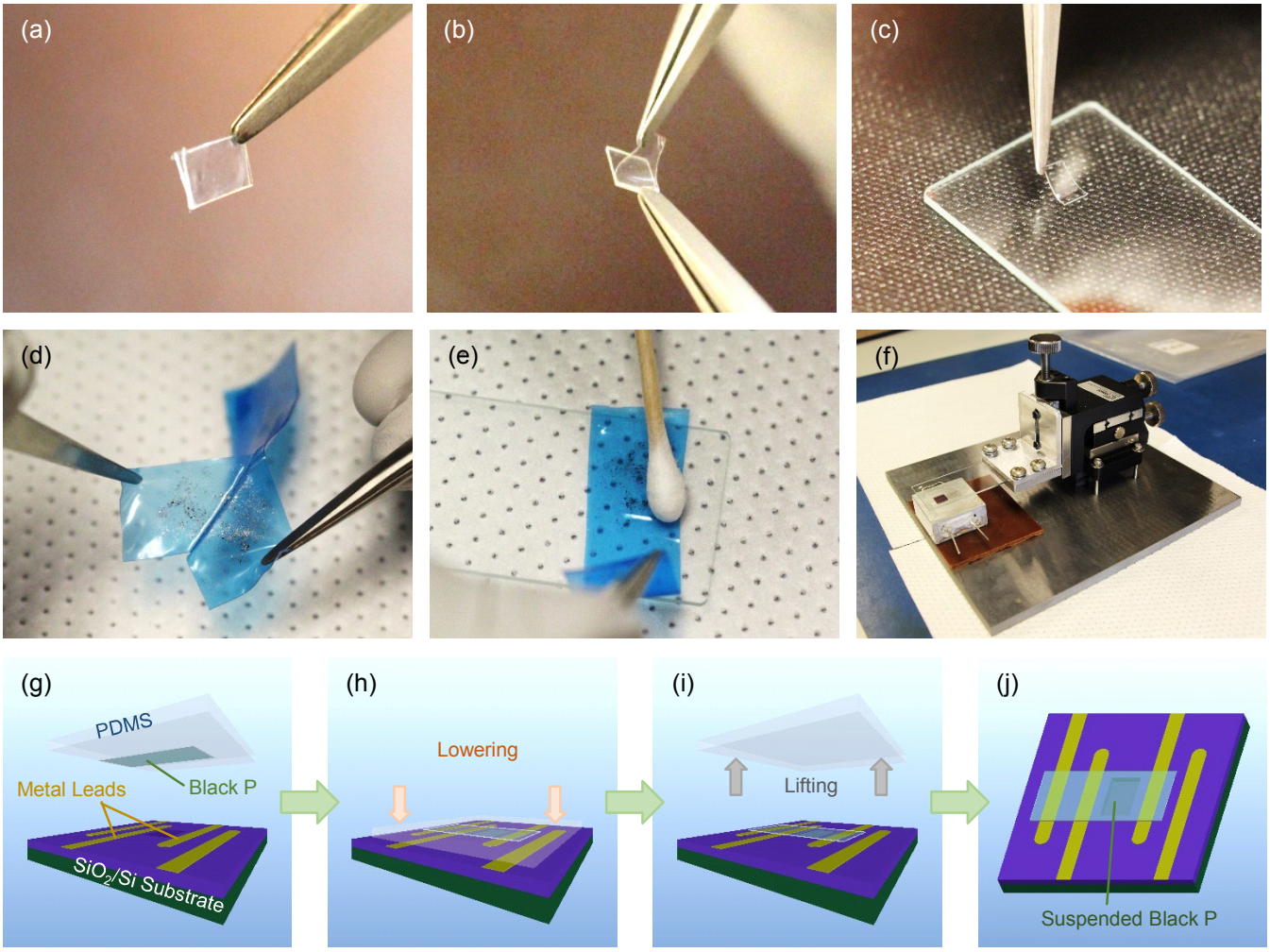

Figure S1: Fabrication process of suspended black P nanoelectromechanical resonators. (a-f) Images of black P flakes exfoliation and transfer preparation steps. (a) PDMS covered with protection layers on both side. (b) Peeling off the protection layers. (c) Applying the PDMS stamp onto a glass slide. (d) Pre-exfoliation of black P. (e) Final exfoliation onto PDMS stamp. (f) Transfer stage with substrate mounted and glass slide clamped. (g-j) Schematic of the transfer process. (g) Aligning the black P flake on PDMS to the prefabricated substrate patterns. (h) Lowering the PDMS stamp to bring the black P flake and substrate into contact. (i) Lifting up the PDMS stamp with the black P flake remaining on the substrate. (j) The resulting device.

S2. Fitting the Data of Thermomechanical Resonance

The signal measured on the spectrum analyzer takes form of a resonance response on top of a frequency-dependent background (see Fig. 2b in the main text). In the frequency domain, the thermomechanical motion of a resonator is given by[4]

$$S_{x,th}^{1/2}(\omega)=\left[\frac{4\omega_0 k_B T}{QM_{eff}}\cdot\frac{1}{\left(\omega_0^2-\omega^2\right)^2+\left(\omega_0\omega/Q\right)^2}\right]^{\frac{1}{2}}, \tag{S1}$$

and simplifies to

$$S_{x,th}^{1/2}(\omega_0)=\sqrt{\frac{4k_B TQ}{\omega_0^3 M_{eff}}}\,. \tag{S2}$$

when the device is on resonance. Here, k_B, T, ω_0, Q, and M_{eff} are the Boltzmann's constant, temperature, angular resonance frequency, quality factor, and the effective mass of the device, respectively.

Assume the noise processes are uncorrelated, the total noise power spectral density (PSD) is the sum of the PSDs from individual noise processes. Thus we have $S_{v,total}^{1/2}=\left(S_{v,th}+S_{v,sys}\right)^{1/2}$. Here $S_{v,th}^{1/2}$ is the thermomechanical motion noise spectral density translated into the electronic domain, through the 'displacement-to-voltage' responsivity $\Re \equiv S_{v,th}^{1/2}/S_{x,th}^{1/2}$. The other term, $S_{v,sys}^{1/2}$, is the voltage noise floor of the measurement system, which depends on the details of the detection scheme. Typically we have $S_{v,sys}^{1/2}\approx 0.1\mu\text{V/Hz}^{1/2}$ in the vicinity of 10MHz frequency band, which slightly increases with increasing frequency. The level of $S_{v,sys}^{1/2}$ determines the off-resonance 'baseline' background ($S_{v,total}^{1/2}\approx S_{v,sys}^{1/2}$ off the resonance).

We fit our data to the expression for $S_{v,total}^{1/2}$, by using $S_{v,th}^{1/2} = \Re \times S_{x,th}^{1/2}$ and treating $S_{v,sys}^{1/2}$ as a frequency-dependent function:

$$S_{v,total}^{1/2} = \left(\Re^2 \times S_{x,th} + S_{v,sys}\right)^{1/2} = \sqrt{\Re^2\left(\frac{4\omega_0 k_B T}{QM_{eff}} \cdot \frac{1}{\left(\omega_0^2 - \omega^2\right)^2 + \left(\omega_0\omega/Q\right)^2}\right) + S_{v,sys}} \,. \qquad \text{(S3)}$$

From the fitting we obtain ω_0, Q, and $S_{v,sys}^{1/2}$ (assuming T = 300K). The curve in Fig. 2b of the Main Text shows a fitting to Eq. S3. From the fitting parameters we extract $\Re$, and calculate $S_x^{1/2}$ from $S_v^{1/2}$ (Main Text, Fig. 2b and Fig. 5c right vertical axis).

S3. Fitting the Data of Time-Domain Ring-Down Measurement

In the time domain measurement, we obtain data as shown in Fig. S2a and S2c. To perform the fitting, we use the ring-down part in the curve (Fig. S2b and S2d). The Q valued could be obtained from the envelope of ring-down which is expressed as an exponential term, while the high frequency oscillations of the device are described by a sinusoidal function. The complete fitting function is given by $a(t) = a_0 + A\exp\left(-\frac{\pi f_{res} t}{Q}\right)\sin\left(2\pi f_{res} t + \phi\right)$, where a_0 is the offset of the response, A is the amplitude, f_{res} is the resonance frequency, and ϕ is the initial phase. In its original form, there are five parameters one need to fit at the same time, which makes it extremely challenging. To attack the problem, we first fix f_{res} and Q values, which are obtained from the frequency domain data. We also estimate A from the starting point amplitude of ring-down process, and a_0 is close to 0 in our data (as one would expect from a proper measurement scheme). Upon initializing the parameters, we first perform the fitting and obtain the values of ϕ and a_0. As the fitting converges, we unfreeze A and Q and continue the fitting procedure. Using this method we obtain very good fitting to the experimental data, as shown in the insets of Fig. S2b and S2d, which show the details of small zoom-in time intervals on the entire ring-down curve. We perform fitting to ring-down measurements under bursts with different duration and strength, and obtain similar Q values of 95, in good agreement with the frequency domain measurement.

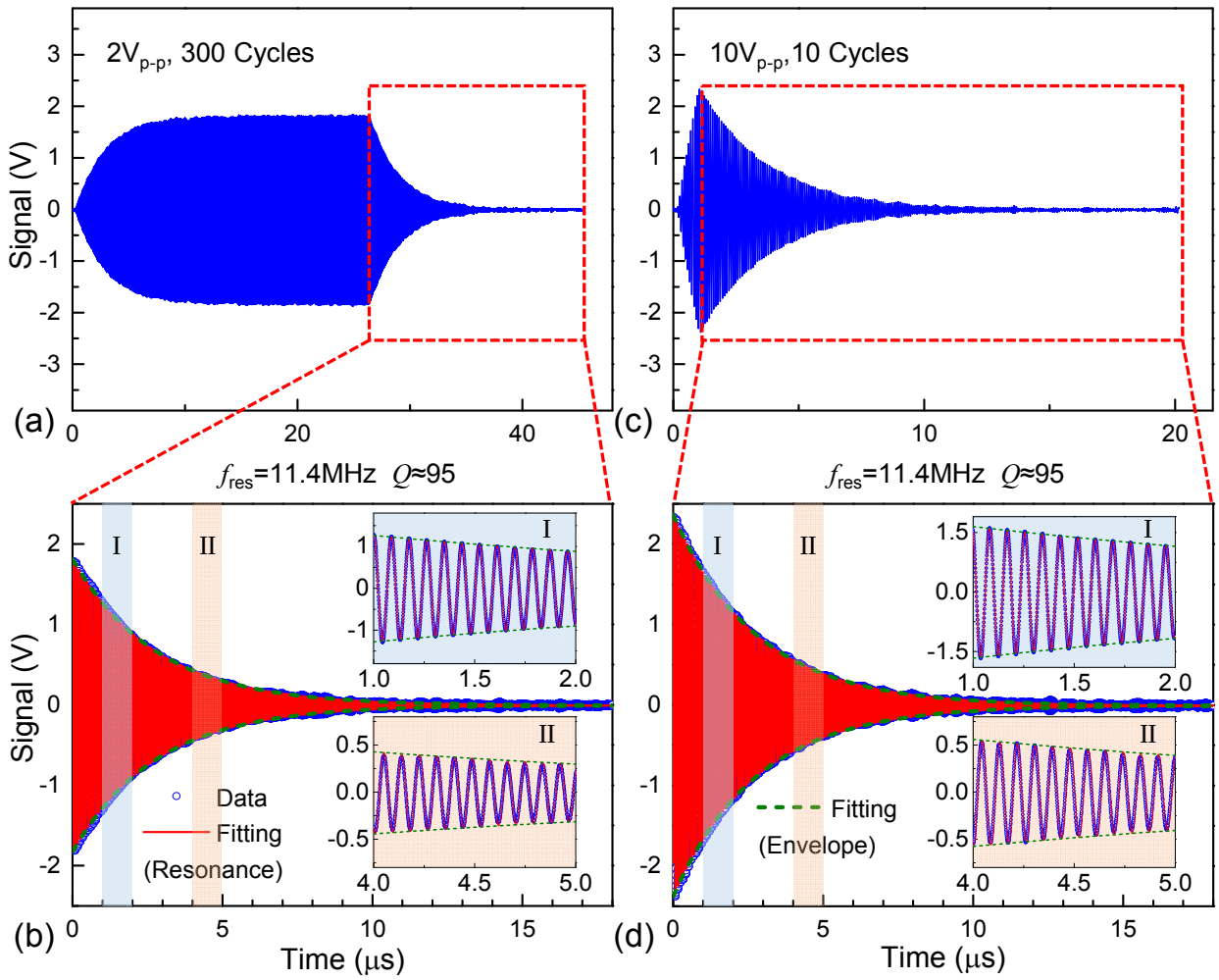

Figure S2: Fitting to the time-domain ring-down measurement. (a) Ring-down data for a 300 cycle burst with amplitude of $2V_{p\text{-}p}$. (b) Fitting to the ring-down data in (a) shown by the red dashed box. (c) Ring-down data for a 10 cycle burst with amplitude of $10V_{p\text{-}p}$. (d) Fitting to the ring-down data in (c) shown by the red dashed box. Insets in (b) and (d) show the zoom-in views of the fitting in the corresponding regions (I and II) as shown by the shaded area in (b) and (d).

S4. Atomic Force Microscope (AFM) Measurement

Because the black P is easily oxidized and we have access to AFM operating in air, the thickness of the devices is measured by AFM after all the measurements are done. We then extract the step heights from the AFM data, as shown in Fig. S3.

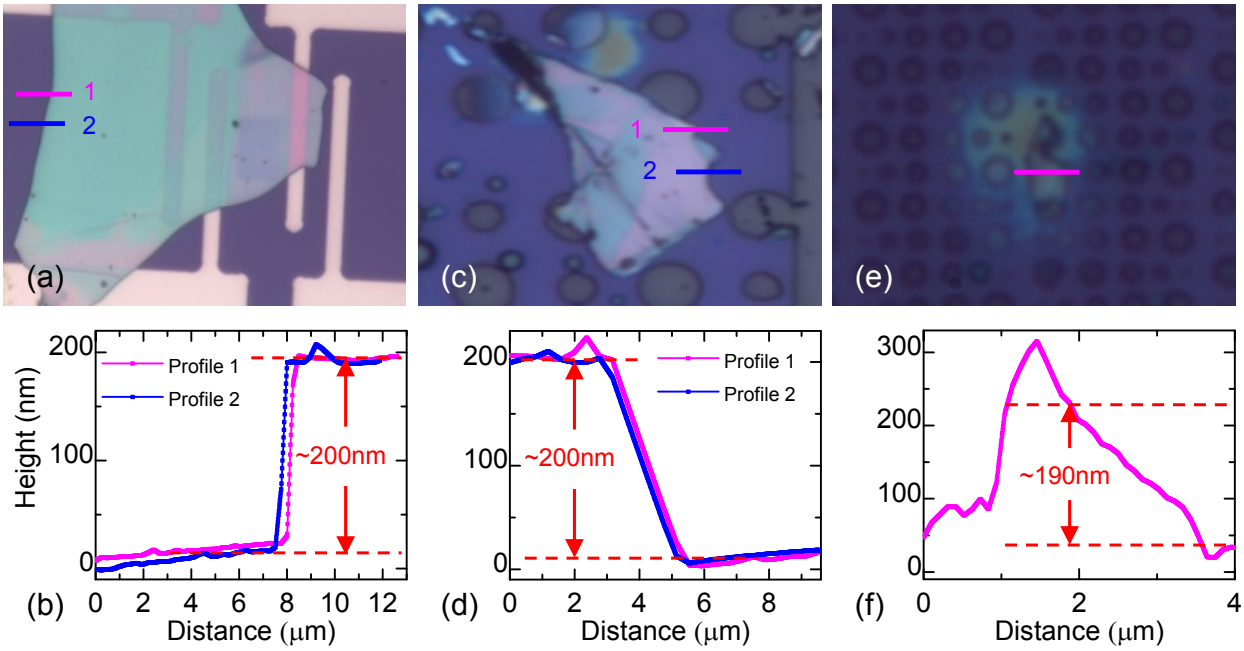

Figure S3: Device thickness measurement with AFM. (a,c,e) Optical microscope images of the devices. (b,d,f) Height measurement of the solid lines indicated in (a), (c), and (e), respectively. (a,b) show the same device in Fig. 1 of Main Text, (c,d) show the device in Fig. 4b and 4d of Main Text, and (e,f) show the device in Fig. 4c of Main Text.

S5. Laser-Induced Degradation of Black P

We observe laser-induced degradation ("laser burning") of black P in optically-driven measurements.

The suspended black P resonator is driven by a modulated 405nm blue laser. We set the DC bias of the laser modulator at 30%, corresponding to an output power of 0.66mW into the microscope, and achieve 100% modulation (amplitude of AC signal equals to DC level) by adjusting the modulation depth and driving signal amplitude. The resonance of the suspended black P resonator is detected interferometrically with a 633nm red laser focused on the surface with <0.7mW on-device power.

Figure S4 shows the "laser burning" process of a black P flake. This black P flake has a thickness of ~200nm, fully covers a 0.6μm hole in the middle, and partially covers 0.8μm hole on the right and a 1.6μm hole on the bottom (as shown in Fig. 4c in the Main Text). Initial blue and red laser positions are illustrated in Fig. S4a. The blue laser is used to photothermally drive the device, and the red laser is focused at the center of the fully-covered circular area. Figure S4b and c show the obvious "burning" effect when lasers are kept at the initial positions during the measurement. We can clearly observe the expansion of "burning" area induced by the blue laser heating effect. We then change the red laser position measure the different devices on this flake (Fig. S4d-f). The blue laser moves accordingly. We clearly observe additional expansion of the "burning" area. Similar effect has been observed in other devices (Fig. 4d in the Main Text). We note that this is the first time that such laser-induced degradation in black P is observed and reported. While additional studies are needed to fully understand and quantify this effect, our results show that laser power should be carefully controlled to limit the heating effect during optical measurements of black P.

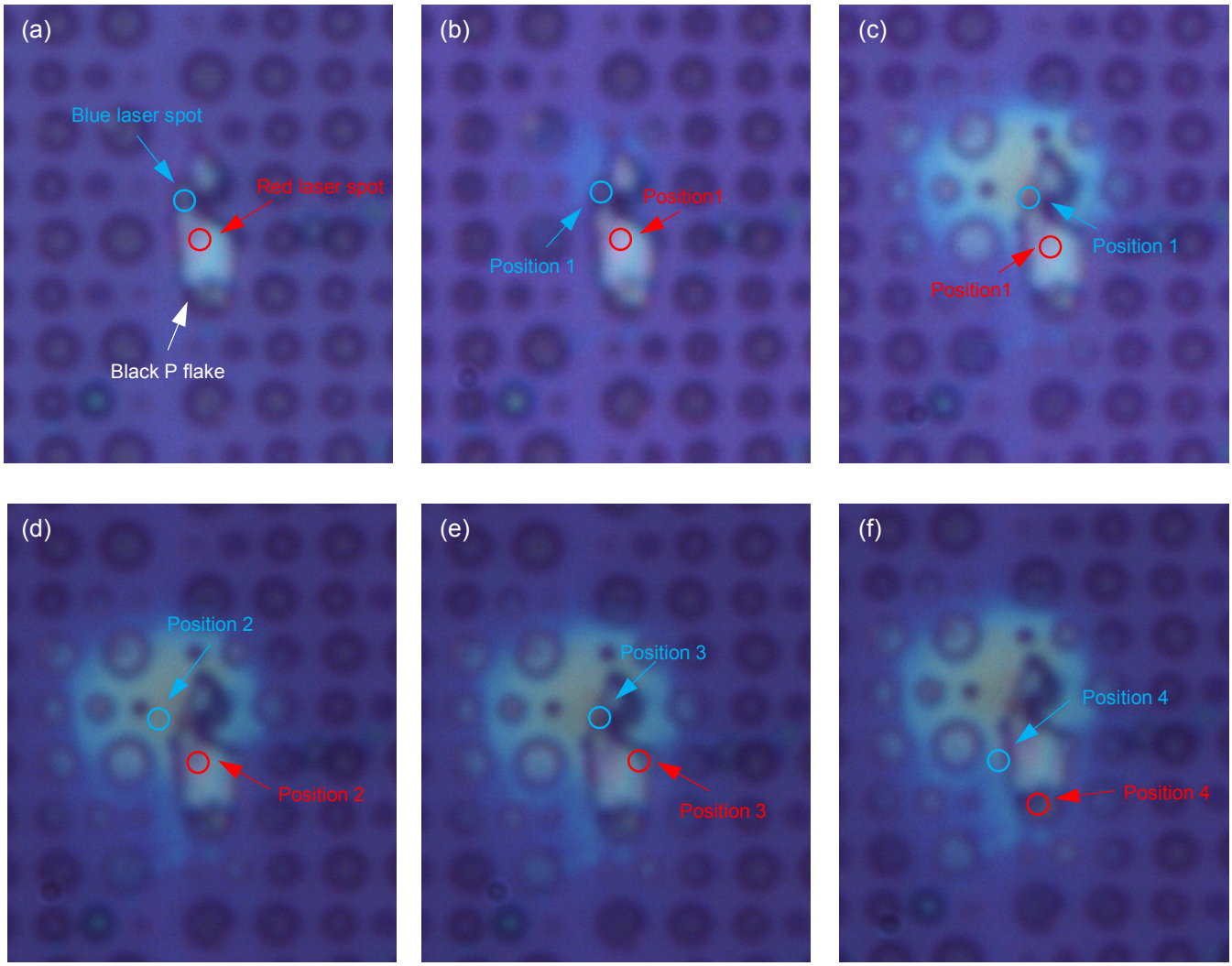

Fig. S4. Laser-induced black P degradation during optically-driven resonance measurement. (a) A black P flake fully covering a 0.6μm circular trench in the middle and partially covering a 0.8μm circular trench on the right and a 1.6μm trench on the bottom. Initial positions of the driving (blue) and detecting (red) lasers are indicated by the blue and red circles. (b) and (c) show increased "burning" by continuous heating of blue laser at the initial position during the measurement. (d), (e) and (f) show further spreading of "burning" area along with the blue laser when lasers are moved to different positions during the measurement.

References

[1] Dean, C. R.; Young, A. F.; Meric, I.; Lee, C.; Wang, L.; Sorgenfrei, S.; Watanabe, K.; Taniguchi, T.; Kim, P.; Shepard, K. L.; Hone, J. Boron Nitride Substrates for High-Quality Graphene Electronics. *Nat. Nanotech.* **2010**, *5*, 722–726.

[2] Wang, L.; Meric, I.; Huang, P. Y.; Gao, Y.; Tran, H.; Taniguchi, T.; Watanabe, K.; Campos, L. M.; Muller, D. A.; Guo, J.; Kim, P.; Hone, J.; Shepard, K. L.; Dean, C. R. One-Dimensional Electrical Contact to a Two-Dimensional Material. *Science.* **2013**, *342*, 614-617.

[3] Castellanos-Gomez, A.; Buscema, M.; Molenaar, R.; Singh, V.; Janssen, L.; van der Zant, H. S. J.; Steele, G. A. Deterministic Transfer of Two-dimensional Materials by All-Dry Viscoelastic Stamping. *2D Mat.* **2014**, *1*, 011002.

[4] Cleland, A. N. *Foundations of Nanomechanics: from Solid-State Theory to Device Applications*. Springer, New York, 2003.